Dynamics of spherical tokamaks with a plasma center column

Pablo L. García-Martínez[1], Leandro G. Lampugnani[1,2] and Ricardo Farengo[2]

[1] *CONICET, Centro Atómico Bariloche, Bariloche, Argentina*

[2] *CNEA and Instituto Balseiro, Centro Atómico Bariloche, Bariloche, Argentina*

Spherical tori or tokamaks (ST) have a number of attractive physical features. From the perspective of reactor engineering design, it would be advantageous if a plasma center column (PCC) can be used in place of the material central post. Biased electrodes across the PCC would drive a plasma current to produce the toroidal magnetic field [1, 2]. With this approach, configurations which share many features with typical ST's, thus called ST-PCC configurations [2], could be formed inside simply connected chambers by driven relaxation [3]. Previous works have focused on the design of the configuration, computation of the equilibrium fields and some preliminar stability analysis based either on the relaxation principle [2] or a linear magnetohydrodynamic (MHD) model [1]. In this paper, we study the dynamics of sustainment of ST-PCC configurations when magnetic helicity is injected using tangential boundary flows. This is done by numerically solving the nonlinear MHD equations in three spatial dimensions. Different distributions of flux across the electrodes are considered, including the plasma gun and the flux core geometries. Three regimes of sustainment with distinct dynamical features are recognized. For the flux core geometry, the periodic formation of tokamak like profiles followed by sudden relaxation events (crashes) is observed.

For the present study, we employ a cylindrical flux conserver, having a pair of concentric electrodes at the bottom and a single electrode at the top. The height of the cylinder is equal to its radius a, and distances are normalized with a. The external magnetic flux (ψ_0) enters through the central electrode at the bottom ($r < 0.4$), a fraction leaves through the upper electrode and the rest through the annular electrode at the bottom end. The three configurations considered are shown in Fig. 1: (a) the plasma gun geometry, where no flux leaves through the upper electrode, (b) the combined case, where half of the flux leaves through the upper electrode and the rest through the annular electrode at the bottom and (c) the flux core geometry, where all the flux leaves through the upper electrode. For each case, the equilibrium configuration, used as the initial condition in the simulations, corresponds to the fully relaxed state given by

$$\nabla \times \mathbf{B} = \lambda \mathbf{B} \quad \text{on } \Omega, \qquad \text{and} \qquad \mathbf{B} \cdot \hat{\mathbf{n}}|_{\partial\Omega} = \mathscr{B}_0, \tag{1}$$

where λ is a constant and $\mathscr{B}_0$ is the normal field across the electrodes. Since in open configurations λ is a free parameter that controls the flux amplification factor ψ_{ma}/ψ_0, where ψ_{ma} is the

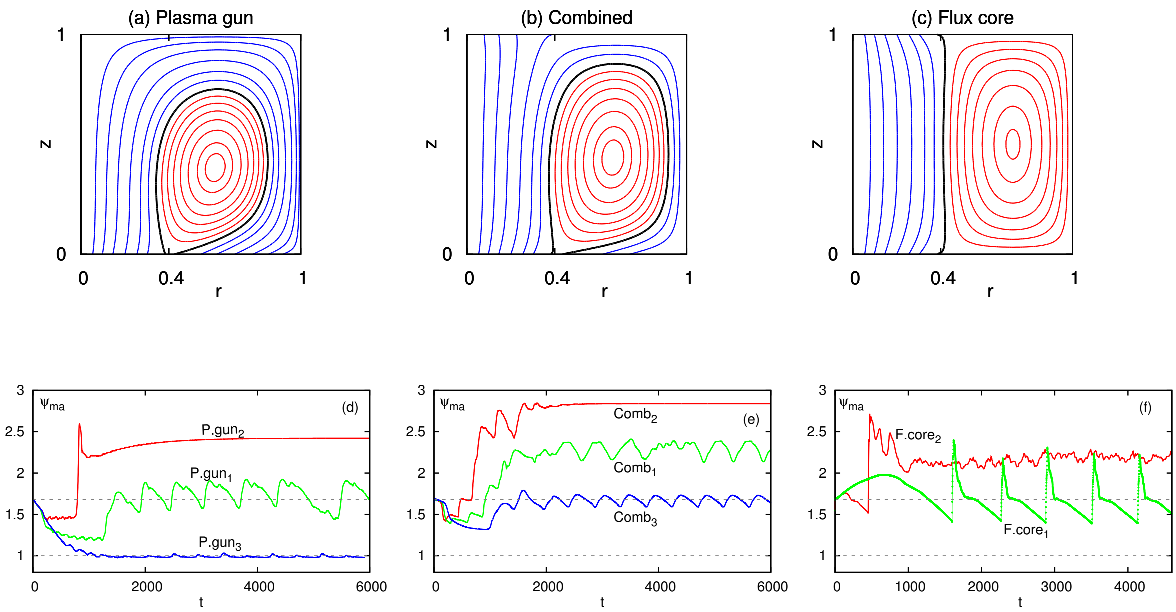

Figure 1: Contours of the poloidal flux of the three studied configurations: (a) plasma gun, (b) combined and (c) flux core. Blue (red) lines indicate the open (closed) flux surfaces. (d)-(f) Evolution of the flux amplification factor (ψ_{ma}) of each configuration for different helicity injection rates.

poloidal flux at the magnetic axis, we set λ to obtain $\psi_{ma}/\psi_0 \approx 1.7$. In what follows, fluxes are normalized with ψ_0, therefore, ψ_{ma} is equal to the flux amplification factor.

The evolution of these configurations is computed using the resistive MHD model as described in Refs. [4, 5]. The resistivity is set to obtain a Lundquist number $S = 4000$ and the magnetic Prandtl number is set to one. To balance the resistive decay, a toroidal velocity profile is imposed at the lower central electrode, where the magnetic flux enters. The velocity is set to zero in the rest of the boundary. This boundary condition drives a poloidal current along the PCC and injects helicity and energy. Since the amount of flux entering through the central electrode at the bottom is fixed, the helicity injection rate is controlled by the magnitude of the imposed toroidal flow. For each configuration, three cases with different helicity injection rates are considered: first, $\dot{H}_1^{inj}$ is set to approximately maintain the initial flux amplification factor of the plasma gun configuration [green lines in Fig. 1 (d)-(f)], then, $\dot{H}_2^{inj} = 2\dot{H}_1^{inj}$ [red lines in Fig. 1 (d)-(f)] and finally, $\dot{H}_3^{inj} = \dot{H}_1^{inj}/2$ [blue lines in Fig. 1 (d) and (e)].

The evolution of ψ_{ma} obtained for the different cases is shown in Fig. 1 (d)-(f). Time is normalized to the Alfvén time. Note that the boundary condition imposed acts as a source of toroidal flux. Therefore, the fact that ψ_{ma} is sustained against resistive dissipation clearly reveals the presence of a relaxation process that drives toroidal current. In Fig. 1 (d)-(f), three different dy-

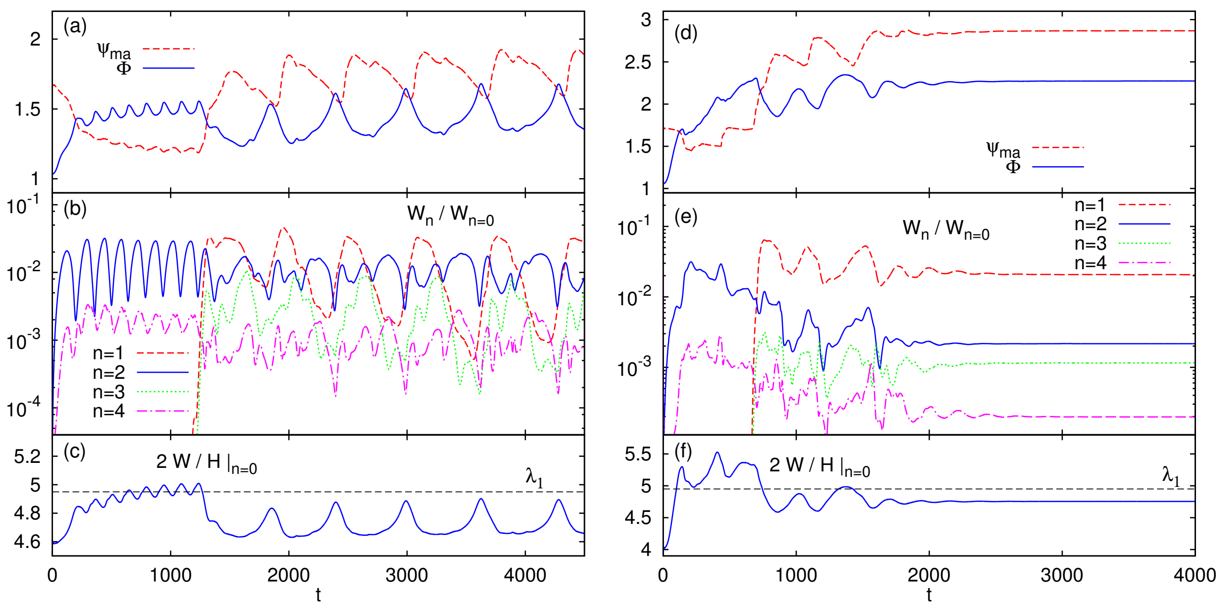

Figure 2: Evolution of (a) the poloidal and toroidal fluxes, (b) the relative magnetic energy of the four dominant modes, and (c) twice the energy to helicity ratio for the P.gun$_1$ case. The evolution of the same quantities for the Comb$_2$ case is shown in (d), (e) and (f).

namical regimes of sustainment can be observed: first, a fluctuating quasi-steady (FQS) regime, e.g. P.gun$_1$, Comb$_1$, Comb$_3$ and F.core$_2$; second, a saturated steady (SS) regime, e.g. P.gun$_2$ and Comb$_2$; third, a periodic full relaxation (PFR) regime, e.g. F.core$_1$. The F.core$_3$ case is not shown because the relaxation process was not triggered within the simulation time.

Fig. 2 shows the evolution of three relevant aspects of the relaxation process: the flux conversion (from toroidal to poloidal), the relative magnetic energy of the four dominant toroidal modes, and (twice) the ratio of magnetic energy to helicity, for the P.gun$_1$ case (left) and the Comb$_2$ case (right). Similar dynamical behaviors were observed in the past [4, 5, 6].

Fig. 3 shows the evolution of (a) the flux conversion, (b) the relative energy spectrum and (c) the energy to helicity ratio for the PFR regime (F.core$_1$ case). This regime is characterized by a slow almost axisymmetric evolution (ramp up phase) followed by a sudden full relaxation event (crash). This behavior is reminiscent of the sawtooth oscillations in tokamaks. Fig. 3 also shows the radial profiles of (d) the magnetic field, (e) the quantity $\mathbf{J}\cdot\mathbf{B}/B^2$ and (f) the safety factor, q. During the ramp up phase, from $t_1 = 3000$ to $t_2 = 3460$, there is a high current density along the open field lines. In the closed flux region, the current profile evolves from a flat profile (green line) to a peaked one (blue line). Remarkably, this almost axisymmetric process produces a tokamak like q profile in the toroidal pinch [blue line in Fig. 3 (f)]. When the parallel current along the last closed surface becomes zero, a full relaxation event is triggered and the

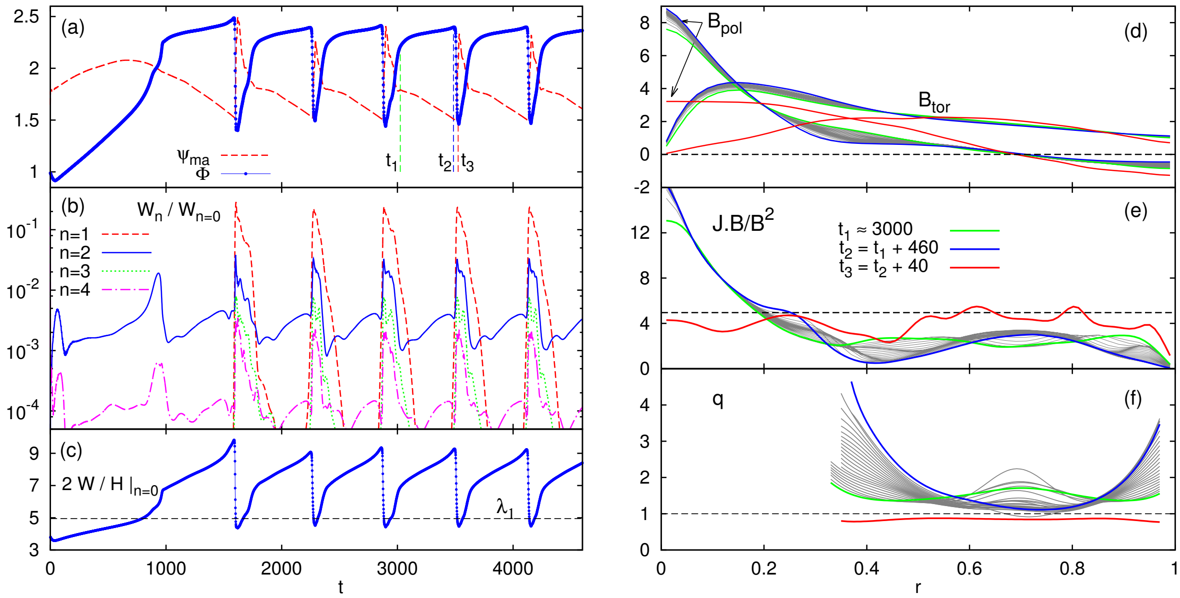

Figure 3: (a) Poloidal and toroidal fluxes, (b) relative magnetic energy spectrum and (c) energy to helicity ratio for the PFR regime (F.core$_1$). (d) Radial profiles of the magnetic field, (e) $\mathbf{J}\cdot\mathbf{B}/B^2$ and (f) q. Gray lines show several instantaneous profiles for times between t_1 and t_2.

configuration rapidly adopts the typical structure of a flux core spheromak (red profiles).
In conclusion, we have studied the dynamics of sustaniment by helicity injection of ST-PCC configurations, taken into account different distributions of the external flux across the electrodes (plasma gun, flux core and combined) and different helicity injection rates. We found three distinct dynamical regimes: fluctuating quasi-steady, saturated steady and periodic full relaxation (observed only for the flux core geometry). The most interesting regime is the last one, in which tokamak like profiles are developed in the closed flux region during a ramp up phase. This relatively slow and almost axisymmetric process is suddenly ended by a rapid full relaxation event (crash) which drives the system back to a typical flux core spheromak configuration.

References

[1] F. Alladio *et al.*, Phys. Plasmas **12**, 112502 (2005).

[2] X. Tang and A. Boozer, Phys. Plasmas **13**, 042514 (2006).

[3] J. B. Taylor, Rev. Mod. Phys. **58** 741 (1986)

[4] P. Garcia-Martinez and R. Farengo, Phys. Plasmas **13**, 042514 (2010).

[5] P. Garcia-Martinez, L. Lampugnani and R. Farengo, Phys. Plasmas **13**, 042514 (2014).

[6] C. Sovinec, J. Finn and D. del-Castillo-Negrete, Phys. Plasmas **8**, 475 (2001).